Photonic-band-structure calculation of material possessing Kerr nonlinearity

P. Tran
Research and Technology Division, Naval Air Warfare Center Weapons Division, China Lake, California 93555
(Received 17 April 1995)

A technique for calculating the photonic band structure of a photonic crystal possessing Kerr nonlinearity and a calculation for a two-dimensional system that shows shifting of the band gap due to the nonlinearity are presented.

The free-photon dispersion can be greatly modified in the presence of a periodic structure. The search for a structure that possesses gaps in the photonic dispersion has received a lot of attention because it is predicted that many new physical phenomena can occur in such a structure, including inhibition of spontaneous emission,[1] strong localization of light,[2] and a photon-atom bound state.[3] Quite a few theoretical techniques have been applied to calculate the photonic band structure. Many of these were developed originally for electronic-band-structure calculations. The plane-wave expansion,[4–6] the Korringa-Kohn-Rostoker (KKR) method,[7,8] the on-shell theory of electron diffraction,[9] and the $\mathbf{k}\cdot\mathbf{p}$ method[10] are a few examples. These methods, however, are not suitable for a photonic crystal that possesses nonlinearity. It is of great interest to have a method for calculating the photonic band structure of a periodic structure possessing nonlinearity since many interesting and useful phenomena such as second-harmonic generation and solitons can occur with nonlinear interaction.

Winful, Marburger, and Garmire[11] have shown that optical bistability can occur in nonlinear-distributed feedback structures. Later Chen and Mills[12] demonstrated, through a numerical study, the existence of a gap soliton in a one-dimensional superlattice, and that the gap soliton plays a key role in the switch from a low- to a high-transmissivity state of the superlattice. Mills and Trullinger[13] subsequently obtained an analytical description of the nonlinear equation of the gap soliton. Recently, John and Akozbek,[14] through a variational technique, predicted the existence of a gap soliton in a two-dimensional (2D) periodic structure. Yablonovitch[15] has discussed the many possible applications of photonic materials, with a gap mode, such as high-gain cavities. In linear materials, a gap mode is introduced through defects which can be hard to control, particularly for a structure that operates in the optical regime and requires a size of order 10^4 ångstroms. The gap soliton may eliminate the need for defects altogether.

In this paper we present a numerical technique based on the finite-difference time-domain (FDTD) method[16] to calculate the photonic band structure of a dielectric structure possessing Kerr nonlinearity. The FDTD technique has been used extensively by the radar community to calculate the radar scattering cross section of complex objects. Chan *et al.*[17] were the first, to our knowledge, to use this technique for the purpose of photonic-band-structure calculation, but only in the linear regime. The idea of the FDTD technique for photonic-band-structure calculation is very simple. We begin with a field distribution ($\mathbf{B}$ and $\mathbf{E}$) that contains a spectrum of wave vectors $\mathbf{k}$ and integrate the two coupled time-dependent Maxwell's equations to get $\mathbf{B}(\mathbf{k},t)$. We then Fourier transform it to get $\mathbf{B}(\mathbf{k},\omega)$. For a given $\mathbf{k}$, the Maxwell's equations, when integrated, will select the frequency that is permissible. The two coupled Maxwell's equations are

$$-\frac{1}{c}\frac{\partial \mathbf{B}}{\partial t}=\nabla\times\mathbf{E}\ , \tag{1}$$

$$\frac{1}{c}\frac{\partial \mathbf{D}}{\partial t}=\nabla\times\mathbf{B}\ , \tag{2}$$

where c is the speed of light and $\mathbf{D}$ is related to $\mathbf{E}$ through the constitutive relation. Given the initial field, we use Eqs. (1) and (2) to get the field at the next time step. After one time step we need to use the constitutive relation to get the $\mathbf{E}$ field in order to start the time integration again. For the linear case, it is simply

$$\mathbf{D}(\mathbf{r})=\epsilon(\mathbf{r})\mathbf{E}(\mathbf{r})\ , \tag{3}$$

where ϵ is the dielectric constant. In the nonlinear case we will have a different constitutive relation. For a Kerr medium Eq. (3) is replaced by

$$\mathbf{D}=(\epsilon+\chi|\mathbf{E}|^2)\mathbf{E}\ , \tag{4}$$

where χ is the third-order nonlinearity. For this system there is a simple analytical solution for $\mathbf{E}$. First we take the magnitude squared of Eq. (4) to get a cubic equation for $x\equiv|\mathbf{E}|^2$,

$$|\chi|^2x^3+2\,\mathrm{Re}(\epsilon^*\chi)x^2+|\epsilon|^2x-|\mathbf{D}|^2=0\ . \tag{5}$$

The solution to a cubic equation is well known so we will not give it here, but the ability to use an analytical formula saves a lot of computation time. The only question is which root to take. For the case we are considering, where ϵ and χ have the same sign, there is only one real and positive root, so the choice is obvious since x must be real and positive. Once x is obtained the $\mathbf{E}$ field is then given by

$$\mathbf{E}=\frac{\mathbf{D}}{\epsilon+\chi x}\ . \tag{6}$$

The calculation is carried out by putting the system on a three-dimensional (3D) grid of $(N_x\times N_y\times N_z)$ points. The curl is evaluated in $\mathbf{k}$ space. This is more accurate than the finite-difference approximation to the curl that is

normally used in the FDTD method. Furthermore, it eliminates the need for a staggered spatial grid (which adds more complexity to the programming), and the periodic boundary condition is automatically satisfied. For each time step, the calculation goes as follows, for the linear case:

$$\mathbf{B}(\mathbf{k},t+\Delta t)=\mathbf{B}(\mathbf{k},t)-(c\Delta t)i\mathbf{k}\times\mathbf{E}(\mathbf{k},t+\Delta t/2)\ , \tag{7}$$

$$\mathbf{D}(\mathbf{k},t+\Delta t/2)=\mathbf{D}(\mathbf{k},t-\Delta t/2)+(c\Delta t)i\mathbf{k}\times\mathbf{B}(\mathbf{k},t)\ , \tag{8}$$

$$\mathbf{E}(\mathbf{r},t)=\mathbf{D}(\mathbf{r},t)/\epsilon(\mathbf{r})\ . \tag{9}$$

We save $\mathbf{B}(\mathbf{k},t+\Delta t)$ at each time step and repeat. For the nonlinear case, Eq. (9) is replaced by the appropriate equation as discussed above. The split time scheme not only gives better accuracy but also saves memory (no need to keep the field at both the present and the next step). Finally, $\mathbf{B}(\mathbf{k},t)$ is Fourier analyzed to get $\mathbf{B}(\mathbf{k},\omega)$. To ensure that we do not miss any mode due to our finite resolution in ω, we multiply $\mathbf{B}(\mathbf{k},t)$ with a Gaussian in time, which has a width half that of $1/\Delta\omega$ where $\Delta\omega$ is our frequency resolution, to broaden the peaks.

Since we are looking for a source-free solution, our solution must satisfy the two divergence conditions. This, however, does not preclude us from choosing an arbitrary initial condition. The fields at a later time will automatically satisfy the divergence conditions as can be seen by taking the divegence of Eqs. (1) and (2). Those of the initial fields that have nonzero divergence can be thought of as fields due to static charges and will show up in the spectrum only at $\omega=0$. The resolution ($\Delta\mathbf{k}$ and $\Delta\omega$) of the calculation is limited by the size of the 3D grid and the integration time. Both of these are computer dependent. However, it should be noted that because of the periodic nature of the system we do not have to worry about edge effects and can integate as long as needed to get the desired resolution in ω.

We first show the result in the linear regime for a dielectric medium ($\epsilon=5.0$) with circular holes drilled through. The holes have a radius of $0.5a$ with a being the lattice constant and form a square lattice. The size of the grid that was used in the calculation is ($L_x=10a$, $L_y=10a$, $L_z=1a$). Since the hole is infinitely long we can choose the length along the cylinder axis (z axis) to our convenience. The grid has $150\times150\times5$ points. For the initial conditions we set the electric and displacement fields to zero and chose a random number between 0 and 1 for the magnetic field at each grid point $\mathbf{r}$. We integrated using a time step of $c\,dt=0.02a$. We also used a time step of $0.01a$ to check that the result has converged and found no change in the result. The total integration time is $cT=400a$ for a frequency resolution of $\omega a/2\pi c=0.0025$. In Fig. 1 we compare the band structure for modes with $\mathbf{E}$ along z that was obtained with the FDTD against that of the plane-wave method.[18] We only show the four lowest bands from the FDTD method. A disadvantage of the present method is that the initial wave field must have nonzero overlap with the eigenmodes of the system in order for us to identify the eigenmodes. This problem is clearly seen in Fig. 1 where in the ΓX and ΓM directions the third band is not seen by the FDTD method. Robertson *et al.*[19] also did not see this

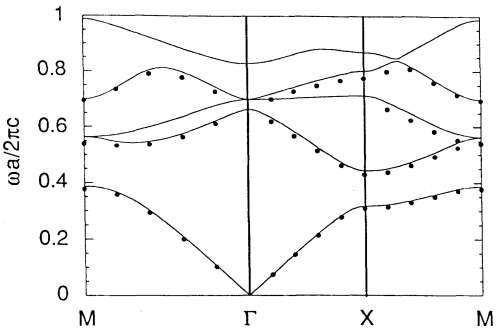

FIG. 1. The photonic band structure of a square lattice of circular holes within a dielectric medium with $\epsilon=5.0$ and $\chi=0$. The radius of the hole is $0.5a$ where a is the lattice constant. The solid line is the plane-wave result. The dots are the FDTD results.

band in their microwave transmission experiment. This is because this band has special symmetry[19] which is not present in the initial wave field. In Fig. 2 we show the spectral plot $|B_x(\omega)|^2+|B_y(\omega)|^2$ as a function of ω for fixed $\mathbf{K}$, along the ΓM and ΓX directions from which we identified the modes shown in Fig. 1. The number beside each peak identifies the point along each direction starting from the Γ point. For example, the number 1 means that it is the first dot on either the left or right of the Γ point in Fig. 1. The relative position of the numbers is meant to indicate the relative position of the peaks since some peaks are not quite visible on the plot. We note that the spectrum is very clean (almost no noise) in the linear regime such that extremely weak peaks can still be identified if the scale is magnified. We get the same band structure using a sum of plane waves [see Eq. (10)] as the initial conditions.

Next we show the result for the same system but with $\chi=0.005$. The following initial conditions were used:

$$\mathbf{B}(\mathbf{r})=\mathbf{D}(\mathbf{r})=\frac{s}{\sqrt{L_xL_yL_z}}\left[\sum_{K\le K_{\max}}e^{i\mathbf{K}\cdot\mathbf{R}}\right](\hat{\mathbf{x}}+\hat{\mathbf{y}}+\hat{\mathbf{z}})\ , \tag{10}$$

where $\mathbf{R}=(x,y)$, s is a scaling factor, and $K_{\max}=2\pi N_x/8L_x$. The initial $\mathbf{E}$ field is obtained from the $\mathbf{D}$ field through Eq. (4). Note that we assign the $\mathbf{D}$ field and then obtain the $\mathbf{E}$ field rather than the other way. If the order were reversed the $\mathbf{D}$ field would have components with wave vector larger than $K_{\max}$ because of the nonlinear operation to get $\mathbf{D}$ from $\mathbf{E}$. The quantity

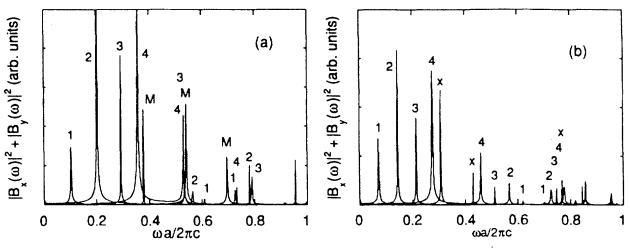

FIG. 2. The spectra, from which the band structure of Fig. 1 is obtained, along the ΓM (a) and ΓM (b) directions.

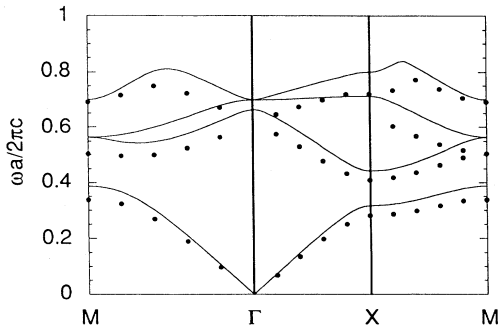

FIG. 3. Same as Fig. 1 but with $\chi=0.005$. For comparison purposes, the plane-wave result for $\chi=0$ is also shown (solid lines).

$2\pi N_x/L_x$ is just the largest wave vector that the fast Fourier transform can resolve in the x direction; therefore the restriction on the sum over $\mathbf{K}$ is to prevent any possible aliasing effect. Another reason for using the sum of plane waves is that the nonlinearity is a function of $\chi|\mathbf{E}|^2$, as can be seen from Eq. (4), so we want an initial field with known characteristics. The scaling factor s is a parameter to control the field intensity at fixed χ. The integration time is $cT=2000a$ for a resolution of $\omega a/2\pi c=0.005$. In Fig. 3 we show the band structure

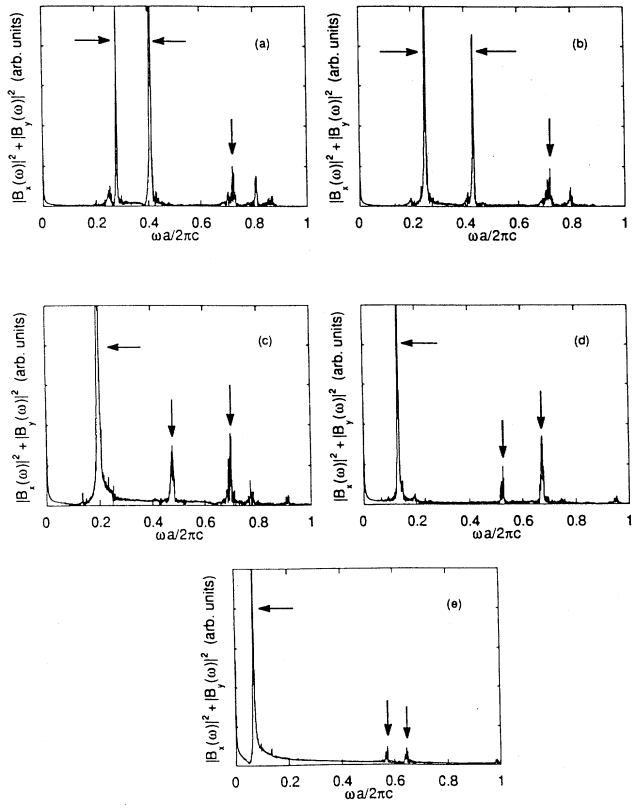

FIG. 4. The spectra corresponding to Fig. 3 along the ΓX direction starting from X point (a) moving toward the Γ point (e).

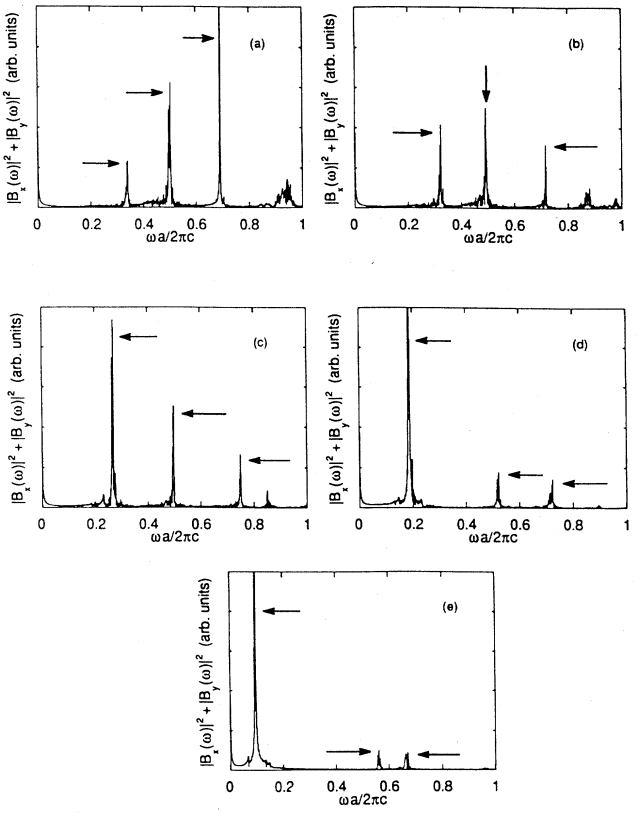

FIG. 5. Same as Fig. 4 but along the ΓM direction starting from the M point (a).

for $s=5.0$. For reference we also show the result obtained by plane-wave expansion in the linear case. The band structure has shifted to lower energy compared to the linear case. This system has an indirect band gap, and the shifting of the band gap as a function of non-

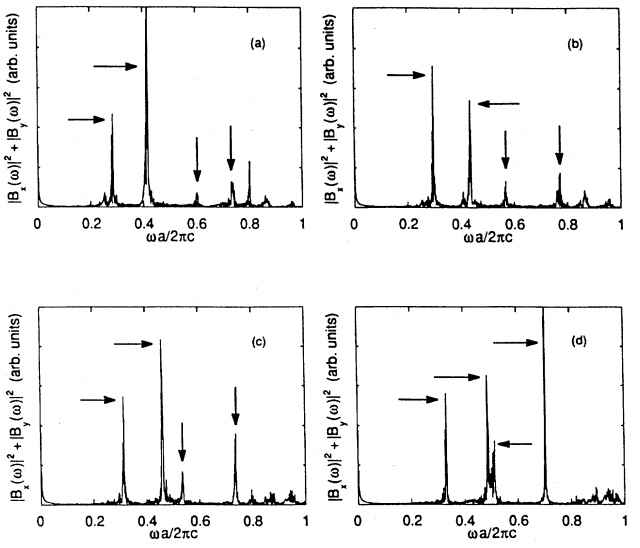

FIG. 6. Same as Fig. 4 but along the XM direction.

linearity may be useful as an optical switching device. In Figs. 4–6 we show the spectra in the ΓX, ΓM, and XM directions, respectively. The spectrum in this case is noisier compared to the linear case. The band structure presented in Fig. 3 is obtained by identifying the modes that exist in the linear case. These are marked by arrows in the spectral plots. In addition to these modes there are other peaks in the spectral plot that we have not been able to identify as different modes or just noise; see, for example, the small peak at $\omega=0.24$ in Fig. 4(a). We also do not know the cause for noise in the case.

In conclusion we have presented a method for calculating the photonic band structure of a nonlinear Kerr photonic crystal. This method does not use the slowly varying envelope approximation. The calculation for a 2D system shows a shifting of the band structure. The shifting of the band gap as a function of the field intensity may be useful as an optical switching mechanism. Further investigation is needed to look for the gap soliton predicted by John and Akozbek.[14]

This work was supported by the Office of Naval Research Code No. 1121RS and the Office of Naval Technology/American Society for Engineering Education.

[1]E. Yablonovitch, Phys. Rev. Lett. **58**, 2059 (1987).
[2]S. John, Phys. Rev. Lett. **58**, 2486 (1987).
[3]S. John and J. Wang, Phys. Rev. Lett. **64**, 2418 (1990).
[4]K. M. Leung and Y. F. Liu, Phys. Rev. Lett. **65**, 2646 (1990).
[5]Z. Zhang and S. Satpathy, Phys. Rev. Lett. **65**, 2650 (1990).
[6]K. M. Ho, C. T. Chan, and C. M. Soukoulis, Phys. Rev. Lett. **65**, 3152 (1990).
[7]K. M. Leung and Y. Qiu, Phys. Rev. B **48**, 7767 (1993).
[8]X. Wang, X.-G. Zhang, Q. Yu, and B. N. Harmon, Phys. Rev. B **47**, 4161 (1992).
[9]J. B. Pendry and A. MacKinnon, Phys. Rev. Lett. **69**, 2772 (1992).
[10]N. F. Johnson and P. M. Hui, Phys. Rev. B **48**, 10 118 (1993).
[11]H. G. Winful, J. H. Marburger, and E. Garmire, Appl. Phys. Lett. **35**, 379 (1979).
[12]W. Chen and D. L. Mills, Phys. Rev. Lett. **58**, 160 (1987).
[13]D. L. Mills and S. E. Trullinger, Phys. Rev. B **36**, 947 (1987).
[14]S. John and N. Akozbek, Phys. Rev. Lett. **71**, 1168 (1993).
[15]E. Yablonovitch, J. Phys. Condens. Matter **5**, 2443 (1993).
[16]K. S. Yee, IEEE Trans. Antennas Propag. **AP-14**, 302 (1966).
[17]C. T. Chan, K. M. Ho, C. M. Soukoulis, S. Datta, and C. L. Yu (unpublished); C. T. Chan, S. Datta, Q. L. Yu, M. Sigalas, K. M. Ho, and C. M. Soukoulis, Physica A **211**, 411 (1994).
[18]M. Plihal, A. Shambrook, A. A. Maradudin, and P. Sheng, Opt. Commun. **80**, 199 (1991).
[19]W. M. Robertson, G. Arjavalingam, R. D. Meade, K. D. Brommer, A. M. Rappe, and J. D. Joannopoulos, Phys. Rev. Lett. **68**, 2023 (1992).